



Cite this: DOI: 10.1039/d6ob00305b

## Investigations toward a unified reaction pathway of thermal and TBSOTf-mediated oxidopyrylium-alkene (5 + 2) cycloadditions

Adam J. Youman,<sup>a</sup> Samantha N. Rokey,<sup>a</sup> Wentao Guo,<sup>b</sup> Jacob P. Grabowski,<sup>a</sup> Susanna N. Angles,<sup>a</sup> Jacob J. Bulandr,<sup>a</sup> Qing Sun,<sup>b</sup> John R. Goodell,<sup>a</sup> Dean J. Tantillo<sup>b</sup> and T. Andrew Mitchell<sup>\*a</sup>

Oxidopyrylium-based (5 + 2) cycloadditions are crucial reactions to construct seven-membered carbocycles containing an ether bridge (*i.e.* oxabicyclo[3.2.1]octanes). Intramolecular silyloxypyronone-based (5 + 2) cycloadditions were investigated and revealed several features: (1) the TBDPS thermal process proceeds *via* a zwitterionic oxidopyrylium intermediate similar to previously reported TBS variants; (2) the TBSOTf-mediated reaction proceeds through a cationic oxidopyrylium intermediate; (3) quantum chemical calculations predict a stepwise process for an electron-rich dipolarophile for each set of conditions. The thermal silyloxypyronone-based (5 + 2) cycloadditions were extremely dependent on the nature of the dipolarophile and the silyl transfer group. The TBDPS enhances the rate compared to the TBS variant but only for less polarized alkenes. Relatively neutral alkenes were the least reactive for both, whereas electron-deficient and electron-rich dipolarophiles were more reactive providing evidence for ambident oxidopyrylium intermediates. TBSOTf-mediated cycloadditions, however, revealed evidence for a cationic intermediate that follows a more consistent mechanistic trend. Qualitative rate studies, Hammett linear free energy relationships, and theoretical calculations combine to provide evidence for both mechanistic scenarios.

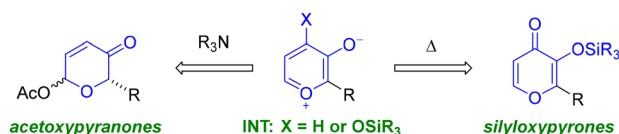
Received 20th February 2026,  
Accepted 16th April 2026

DOI: 10.1039/d6ob00305b

rsc.li/obc

Cycloadditions can be initiated by the input of thermal energy or an activating agent to access key transition states *en route* to a desired product.<sup>1</sup> Oxidopyrylium-based (5 + 2) variants<sup>2</sup> can be mediated by different pathways, but two widely utilized strategies involve acetoxy-pyranones or silyloxypyronones (Scheme 1). Activation of acetoxy-pyranones, established by Hendrickson<sup>3</sup> and Sammes,<sup>4</sup> typically requires a base to initiate deprotonation followed by release of the acetoxy (or related leaving group) to deliver the oxidopyrylium. Activation of silyloxypyronones (or related starting material), pioneered by Wender and Mascareñas,<sup>5</sup> takes advantage of either an internal group transfer process or an external Lewis acid to afford the oxidopyrylium moiety. Several variations of these methods have been reported<sup>6</sup> and our group has contributed to both activation pathways,<sup>7</sup> which are useful toward the total synthesis of natural products<sup>8</sup> and other applications.<sup>9</sup> The generally accepted mechanism<sup>7b,10</sup> involves silyl transfer to the oxidopyrylium followed by concerted cycloaddition. We pre-

viously reported silyloxypyronone-based cycloadditions that revealed crucial data regarding three components: silyl group transfer,<sup>7g</sup> tether proximity to the transfer group,<sup>7g</sup> and dipolarophile electronics.<sup>7b</sup> Relative rate comparisons of a wide variety of silylated maltol-derived substrates **1a–j** revealed an interesting result: only TBDPS-terminal olefin **1b** exhibited enhanced reactivity and transfer group dependence (Scheme 2A).<sup>7g</sup> Furthermore, several silylated kojic acid-derived substrates **3a–d** showed no dependence on the transfer group (Scheme 2B).<sup>7g</sup> Although enoates **1f–j** and **3c–d** were not affected by the silyl transfer group, enhanced conversion was observed compared to the terminal alkenes confirming the expected electronic effect of the ester that reduces the energy of the lowest unoccupied molecular orbital (LUMO). These combined results revealed a subtle interplay between transfer group, tether, and alkene. More recently, we undertook a



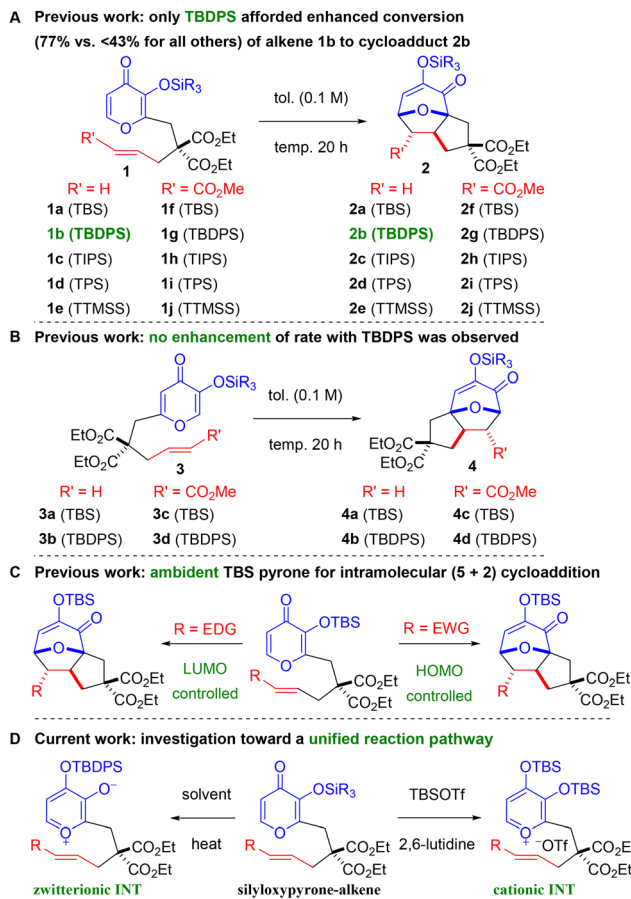
Scheme 1 Acetoxy-pyranone vs. silyloxypyronone activation.

<sup>a</sup>Department of Chemistry, Illinois State University, Campus Box 4160, Normal, IL 61790-4160, USA. E-mail: mitchell@ilstu.edu

<sup>b</sup>Department of Chemistry, University of California, Davis, 1 Shields Avenue, Davis, CA 95616, USA. E-mail: dtantillo@ucdavis.edu

† A. J. Y., S. N. R., and W. G. contributed equally to this research.





**Scheme 2** Summary of transfer group, tether, and dipolarophile effects on silyloxyprone-based (5 + 2) cycloaddition leading to further understanding toward a unified reaction pathway.

detailed investigation of TBS-pyrone that revealed the substantial impact of dipolarophile electronics on the cycloaddition that illuminated a spectrum of reactivity<sup>7b</sup> passing through borderlands<sup>11</sup> of concerted and stepwise (Scheme 2C). Herein, we disclose TBDPS-thermal and TBSOTf-mediated<sup>6o</sup> (5 + 2) cycloadditions that proceed *via* zwitterionic and cationic intermediates, respectively (Scheme 2D). Taken together with our previous work,<sup>7b,g</sup> these qualitative rate studies, Hammett linear free energy relationship (LFER) findings, and theoretical calculations provide a coherent framework for a unified mechanistic pathway of silyloxyprone-based (5 + 2) cycloadditions (*vide infra*) and lay the foundation for continued exploration of this intriguing reaction.

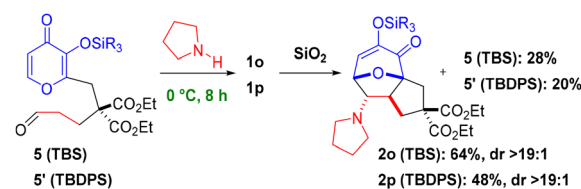
## Results and discussion

Building on the previous observation that the TBDPS transfer group showed no enhancement of enoate conversion (*vide supra*),<sup>7g</sup> we undertook a more thorough comparison of TBS- and TBDPS-pyrone<sup>7b</sup> with a range of substituents on the dipolarophile (Table 1 and Scheme 3). Ambient temperature qualitative rate studies afforded good mass recovery and, as

**Table 1** Qualitative rate comparison of various dipolarophiles in silyloxyprone-based (5 + 2) cycloadditions

Entry	SiR <sub>3</sub>	R'	% rec. <sup>a</sup> ( <b>1</b> )	% yield <sup>a</sup> ( <b>2</b> )
1	TBS <sup>c</sup>	H	>95 ( <b>1a</b> )	<5 ( <b>2a</b> ) <sup>b</sup>
2	TBDPS	H	>95 ( <b>1b</b> )	<5 ( <b>2b</b> ) <sup>b</sup>
3	TBS <sup>d</sup>	CO <sub>2</sub> Me	77 ( <b>1f</b> )	7 ( <b>2f</b> )
4	TBDPS <sup>d</sup>	CO <sub>2</sub> Me	78 ( <b>1g</b> )	8 ( <b>2g</b> )
5	TBS <sup>c</sup>	C(O)Me	54 ( <b>1k</b> )	36 ( <b>2k</b> )
6	TBDPS	C(O)Me	56 ( <b>1l</b> )	37 ( <b>2l</b> )
7	TBS	NO <sub>2</sub>	<5 ( <b>1m</b> ) <sup>b</sup>	73 ( <b>2m</b> )
8	TBDPS	NO <sub>2</sub>	<5 ( <b>1n</b> ) <sup>b</sup>	84 ( <b>2n</b> )

<sup>a</sup> Determined by <sup>1</sup>H NMR analysis using 1,3,5-trimethoxybenzene as an internal standard. <sup>b</sup> Not detected. <sup>c</sup> Previously reported in ref. 7b (*J. Org. Chem.* 2023, **88**, 5972); included for comparison with new TBDPS data. <sup>d</sup> Previously reported in ref. 7g (*J. Org. Chem.* 2019, **84**, 10306); included for comparison with new TBDPS data.



**Scheme 3** Low temperature enamine (5 + 2) cycloaddition (reproduced in part with permission from ref. 7b).

expected, terminal olefins **1a**<sup>7b</sup> and **1b** both afforded no reaction (Table 1, entries 1 and 2). As the electron-withdrawing ability of the substituent increased, enhanced conversion was observed. Enoates **1f–g**<sup>7g</sup> gave minimal conversion (Table 1, entries 3 and 4),<sup>7b</sup> enones **1k**<sup>7b</sup> and **1l**<sup>12</sup> provided more substantial quantities of adducts **2k–l** (Table 1, entries 5 and 6), and nitro-enes **1m–n** afforded complete conversion (Table 1, entries 7 and 8),<sup>12</sup> thus confirming the effect of lowering the energy of the LUMO. These newly reported nitro-ene starting materials **1m–n** and corresponding cycloadducts **2m–n** were less stable than carbonyl substrates **1f–l**. Therefore, we do not believe that conversions of nitro-enes **1m–n** (entries 7 and 8) are reflective of rate enhancement by the TBDPS but rather reveal that the TBDPS is simply more stable and thus both are functioning similarly as transfer groups in the case of electron-poor dipolarophiles. Enamine **1o** was previously reported<sup>7b</sup> to proceed at ambient temperature (*in situ via* aldehyde **5**) and newly investigated variant **1p** further demonstrates that enhancement with the TBDPS transfer group is limited to less polarized alkenes (*vide infra*). Unique parameters were necessary to probe this variant below ambient temperature (Scheme 3). When a cycloaddition proceeds at room temperature, the substrate is likely to continue reacting upon isolation and purification, potentially skewing the results. By simply



passing the reaction mixture over silica gel, *in situ* generation of enamines **1o-p** (not shown) from aldehydes **5/5'** is reversible, and the reaction is quenched. Therefore, enamine **1o** was formed at 0 °C to give cycloadduct **2o** (64% yield) and aldehyde **5** (28% yield) after column chromatography of the reaction mixture.<sup>7b</sup> A similar result in this study was obtained with the TBDPS variant **2p**.<sup>12</sup>

Linear free energy relationship (LFER) studies (*i.e.*, Hammett plots) offer a powerful avenue to probe reaction pathways *via* substituent effects.<sup>13</sup> Plotting the substituent constant ( $\sigma$ ) vs. the corresponding log [ $k/k_0$ ] (or related rate parameter) typically reveals a linear trend that provides support for a consistent mechanism in operation, and non-linear Hammett plots afford compelling evidence for a change in mechanism across substituents.<sup>14</sup> We previously synthesized various styrenes with TBS<sup>7b</sup> (**1q-z**) and herein with TBDPS<sup>12</sup> (**1q'-z'**) transfer groups and subjected them to uniform conditions (Table 2). With both transfer groups, electron-donating and electron-deficient substrates were more reactive than less polarized variants. The TBDPS group slightly enhanced the reactivity as compared to the TBS further indicating that this phenomenon is limited to less polarized alkenes. For example, 4-dimethylaminostyrenes **1q/1q'** (Table 2, entry 1) gave similar conversion as the electron deficient ester-substituted **1x/1x'** (Table 2, entry 8) and 4-cyano-substituted **1y/1y'** (Table 2, entry 9), while the 4-nitrostyrenes **1z/1z'** afforded the highest conversion (Table 2, entry 10). Less-polarized derivatives such as phenyl **1u/1u'** and 4-fluoro **1v/1v'** were far less reactive by comparison (Table 2, entries 5 and 6). When log rate/rate<sub>0</sub> was plotted against  $\sigma_p$  constants, non-linear Hammett plots were revealed (Fig. 1 and 2). These plots are consistent with a shift in reaction pathway with an inflection point near the phenyl

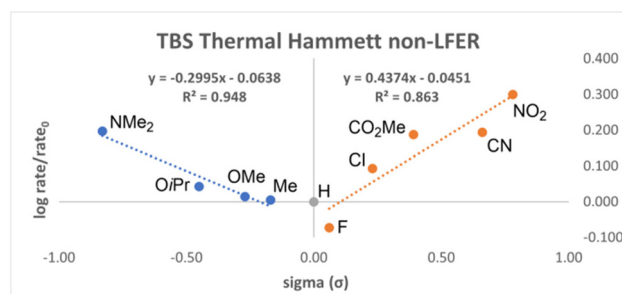


Fig. 1 Hammett analysis: TBS thermal non-LFER (reproduced with permission from ref. 7b; *J. Org. Chem.* 2023, **88**, 5972).

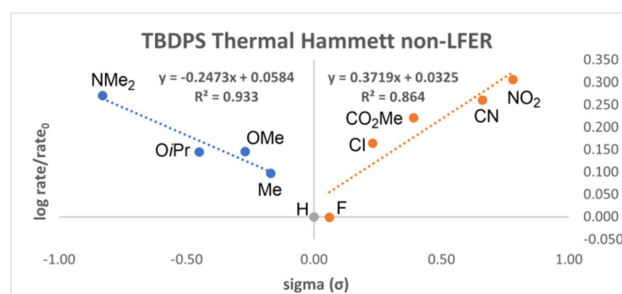
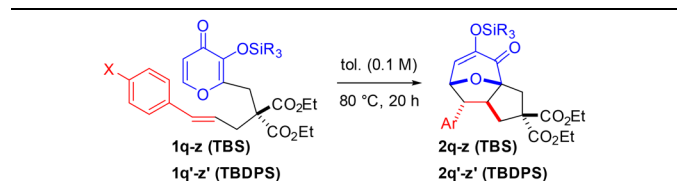


Fig. 2 Hammett analysis: TBDPS Thermal non-LFER.

**1u/1u'** (Table 2, entry 5) and 4-fluoro **1v/1v'** (Table 2, entry 6). In both cases, upon separation of the trendlines by Sigma ( $\sigma$ ) value, two distinctly linear Hammett plots are revealed. The negative slope ( $\rho$ ) correlates to electron-donating group acceleration, whereas electron-withdrawing group acceleration is indicated by the positive slope ( $\rho$ ).

An alternative to thermal-mediated silyl transfer, TBSOTf-promoted (5 + 2) cycloadditions<sup>60</sup> were explored with a subset of styrenes **2s,t,u,w,z** (Table 3) and **4e-i** (Table 4). Due to the proposed cationic intermediate (*cf.* Scheme 2D), these investigations afforded evidence of a more typical mechanistic pathway regardless of dipolarophile electronics. In each series,

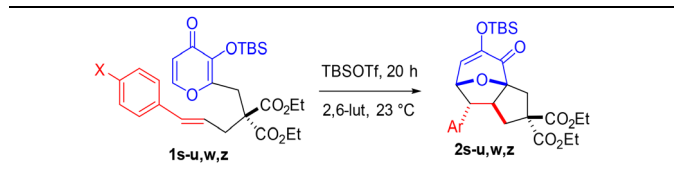
Table 2 Linear free-energy relationship comparison of TBS and TBDPS styrenes (reproduced in part with permission from ref. 7b)



Entry	X	% yield <sup>a</sup> ( <b>2</b> ) <sup>b</sup>	$\sigma_p$	% yield <sup>a</sup> ( <b>2'</b> )
1	NMe <sub>2</sub>	69 ( <b>2q</b> )	-0.83	87 ( <b>2q'</b> )
2	OiPr	48 ( <b>2r</b> )	-0.45	65 ( <b>2r'</b> )
3	OMe	45 ( <b>2s</b> )	-0.27	65 ( <b>2s'</b> )
4	Me	44 ( <b>2t</b> )	0.17	58 ( <b>2t'</b> )
5	H	44 ( <b>2u</b> )	0.00	47 ( <b>2u'</b> )
6	F	37 ( <b>2v</b> )	0.06	46 ( <b>2v'</b> )
7	Cl	54 ( <b>2w</b> )	0.23	68 ( <b>2w'</b> )
8	CO <sub>2</sub> Me	67 ( <b>2x</b> )	0.39	77 ( <b>2x'</b> )
9	CN	68 ( <b>2y</b> )	0.66	85 ( <b>2y'</b> )
10	NO <sub>2</sub>	87 ( <b>2z</b> )	0.78	94 ( <b>2z'</b> )

<sup>a</sup> Determined by the average of two trials as measured by <sup>1</sup>H NMR analysis with 1,3,5-trimethoxybenzene as an internal standard.  
<sup>b</sup> Previously reported in ref. 7b (*J. Org. Chem.* 2023, **88**, 5972); included for comparison with new TBDPS data.

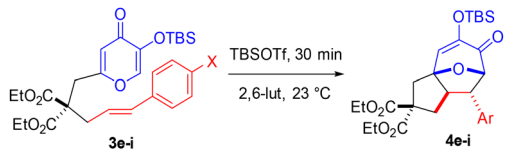
Table 3 Linear free-energy relationship of styrenes with TBSOTf



Entry	X	% conv. <sup>a</sup> ( <b>2</b> )	$\sigma_p^+$	Log (rate/rate <sub>0</sub> )
1	OMe	100 ( <b>2s</b> )	-0.78	0.569
2	Me	98 ( <b>2t</b> )	-0.31	0.560
3	H	27 ( <b>2u</b> )	0.00	0.000
4	Cl	22 ( <b>2w</b> )	0.11	-0.089
5	NO <sub>2</sub>	4 ( <b>2z</b> )	0.79	-0.829

<sup>a</sup> Determined by the average of two trials as measured by <sup>1</sup>H NMR analysis with 1,3,5-trimethoxybenzene as an internal standard.

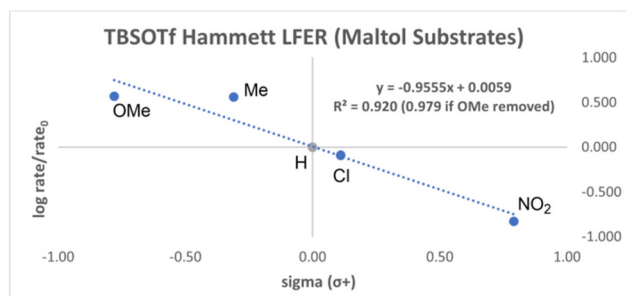
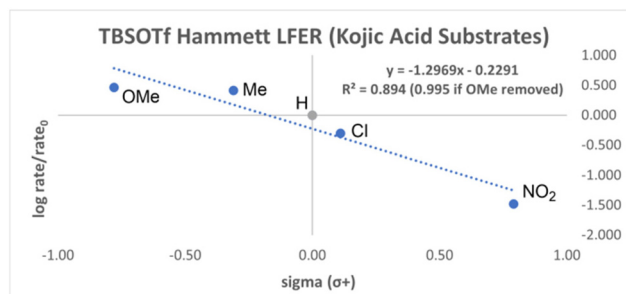


**Table 4** Linear free-energy relationship of styrenes with TBSOTf


Entry	X	% conv. <sup>a</sup> (4)	$\sigma_p^+$	Log (rate/rate <sub>0</sub> )
1	OMe	100 (4e)	-0.78	0.467
2	Me	89 (4f)	-0.31	0.415
3	H	33 (4g)	0.00	0.000
4	Cl	16 (4h)	0.11	-0.301
5	NO <sub>2</sub>	1 (4i)	0.79	-1.480

<sup>a</sup> Determined by the average of two trials as measured by <sup>1</sup>H NMR analysis with 1,3,5-trimethoxybenzene as an internal standard.

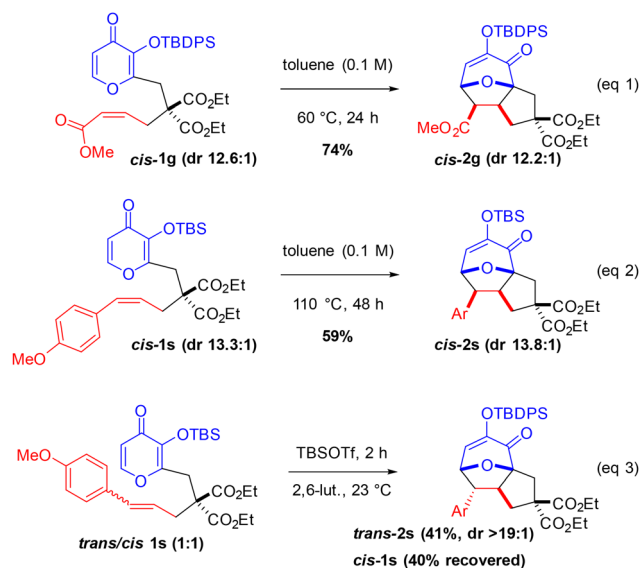
the reaction rate increased with enhanced electron density of the styrene substituent. Kojic acid substrates (Table 4) were more reactive than maltol variants (Table 3), with timeframes of 30 minutes *vs.* 20 hours, respectively. In both cases, Hammett plots revealed a straightforward linear trend (Fig. 3 and 4) providing evidence for a rate-determining transition state involving accumulation of positive charge on the nucleophilic styrene *via* the proposed cationic oxidopyrylium species (*vide supra*). It was a challenge to ascertain an appropriate time course for all substrates since methoxy-substituted styrenes **1s** and **3e** were completely consumed with only minimal conversion of the nitro-substituted styrenes **1z** and **3i**. Thus, the

**Fig. 3** Hammett analysis: TBSOTf (maltol substrates).**Fig. 4** Hammett analysis: TBSOTf (kojic acid substrates).

results were slightly skewed, and the  $R^2$ -value improved upon calculation without the methoxy-substituted styrenes.

To confirm the stereospecific nature of the thermal and TBSOTf-mediated (5 + 2) cycloadditions, two *cis* alkenes **1g** and **1s** were synthesized.<sup>12</sup> Cycloadditions utilizing these *cis* alkenes **1g** and **1s** (Scheme 4) complimented the stereospecific nature that was observed previously with various *trans* olefins.<sup>7b,g</sup> First, enoate *cis*-**1g** underwent smooth cycloaddition at 60 °C with complete stereospecificity (eqn (1)). Styrenes **1s** were subjected to both sets of conditions (*i.e.* thermal and TBSOTf)<sup>12</sup> to investigate relative reactivity and stereospecificity (eqn (2)–(3)). Styrene *cis*-**1s** was significantly less reactive than the corresponding styrene *trans*-**1s** and required increased heating (*i.e.* 110 °C) but afforded *cis*-**2s**, also with complete stereospecificity (eq (2)). To confirm this, a mixture of *trans/cis* (1 : 1) was utilized and, upon heating to only 80 °C, *trans*-**1s** underwent significant conversion, but minimal conversion to *cis*-**2s** was observed (not shown).<sup>12</sup> Upon activation with TBSOTf a similar trend was observed after 2 hours with an initial *trans/cis* ratio of 1 : 1. Nearly complete conversion of *trans*-**1s** (<5% remaining) to *trans*-**2s** (41% yield; maximum 50%) was detected while only trace conversion to *cis*-**2s** (<5%) and nearly complete recovery of *cis*-**1s** (40% yield; maximum 50%) was observed (eqn (3)). Further conversion of *cis*-**1s** under these conditions, albeit slowly, was detected (not shown).<sup>12</sup>

Quantum chemical calculations were undertaken to investigate the mechanism of these silyloxyprone-based (5 + 2) cycloadditions. Initial conformational searches were carried out using XTB-CREST<sup>15</sup> and subsequent density functional theory (DFT) calculations were carried out with Gaussian16.<sup>16</sup> The M06-2X functional with the D3(0) dispersion correction<sup>17</sup> was used to locate stationary points, since this functional is known to perform well for main group thermochemistry and kinetic studies.<sup>18</sup> We employed the 6-31+G(d,p) basis set and the SMD continuum solvation model for geometry optimi-

**Scheme 4** Stereospecific cycloadditions with *cis*-alkenes **1g** per **1s**.

zations.<sup>19</sup> The larger 6-311+G(2df,2p) basis set was used for computing single point energies. Reported Gibbs free energies include thermal corrections from frequency calculations at the M06-2X-D3(0)/6-31+G(d,p) level, which was benchmarked with other functional/basis set combinations to confirm that qualitative conclusions did not change.

For reactions in the absence of TBSOTf, silyl transfer *via* a pentacoordinate species was calculated to be fast and non-rate determining in each case.<sup>7b,12</sup> The overall barrier *via* rate-determining concerted synchronous (5 + 2) cycloaddition for terminal alkene **1a** was predicted to be 1.9 kcal mol<sup>-1</sup> higher in energy than the corresponding synchronous concerted (5 + 2) cycloaddition for terminal alkene **1b** (Fig. 5). These predictions correlate to experimental results in which the TBDPS variant reacts faster than the TBS (*cf.* Scheme 2A), although an even larger difference (2.4 kcal mol<sup>-1</sup>) is predicted for the kojic acid-derived analogs, which is not borne out in experiments (*cf.* Scheme 2B). These results with the TBDPS should be viewed with some caution (the issue is likely related to challenges in modeling the conformational properties of the TBDPS group). Nonetheless, barriers were predicted to be higher for kojic acid-derived substrates than for maltol-derived systems with both TBS (Fig. 5) and TBDPS<sup>12</sup> transfer groups.

Concerted but asynchronous (5 + 2) cycloaddition TSs were found for oxidopyrylium intermediates derived from **1q–z** and the plot of computationally predicted free energy barriers *vs.* substituent constants ( $\sigma_p$ ) was previously shown<sup>7b</sup> to be non-

linear in qualitative agreement with experimental results (*cf.* Fig. 1). The same effect was found for TBDPS-containing systems **1q'**, **1u'**, **1z'** (Fig. 6). Again, lower barriers were predicted for the TBDPS variants by ~2 kcal mol<sup>-1</sup>, reinforcing the influence of this bulkier group on less polarized dipolarophiles. DFT calculations for cationic intermediates derived from TBSOTf show that the methoxy substituent promotes a stepwise (5 + 2) cycloaddition (Fig. 7) while both H and NO<sub>2</sub> substituents promote an asynchronous concerted process.<sup>12</sup>

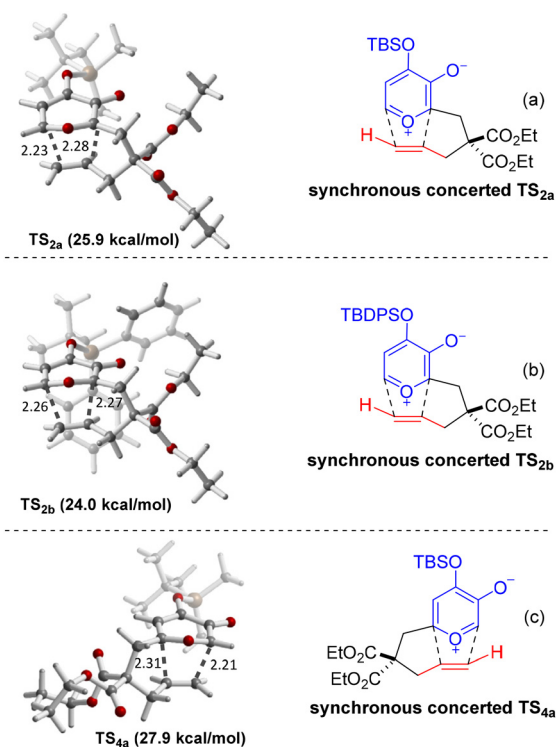


Fig. 5 TSs of (a) maltol-derived terminal olefin (TBS);<sup>7b</sup> (b) maltol-derived terminal olefin (TBDPS); (c) kojic acid-derived terminal olefin (TBS).

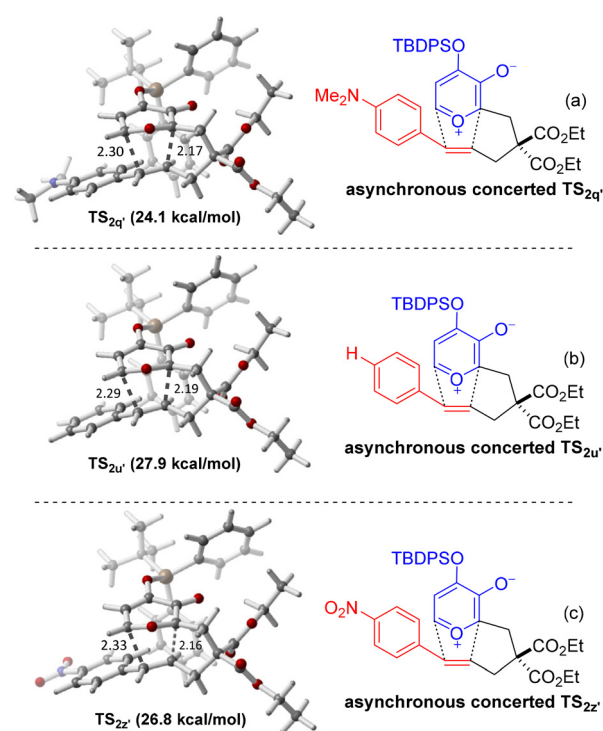


Fig. 6 TSs of (a) dimethylaminostyrene (TBDPS); (b) styrene (TBDPS); (c) nitrostyrene (TBDPS).

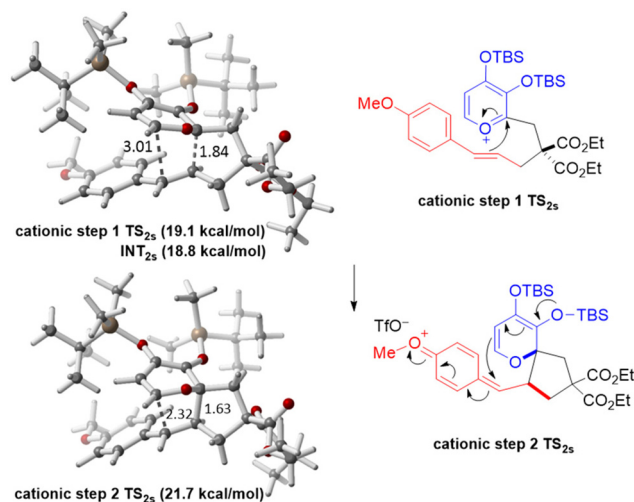


Fig. 7 TSs of stepwise TBSOTf-mediated cationic (5 + 2) cycloaddition of methoxy styrene variant.



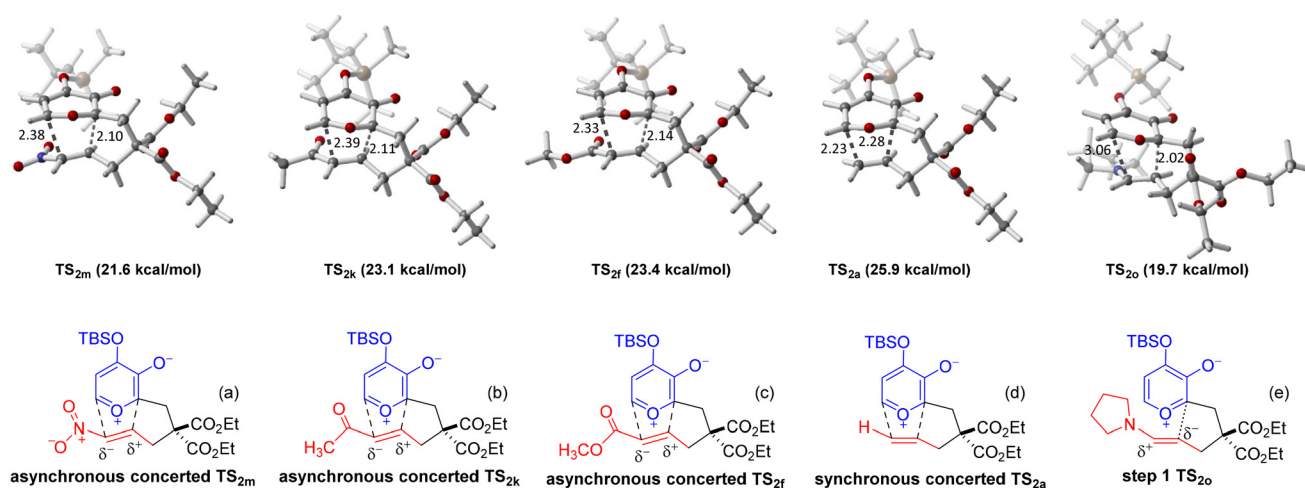
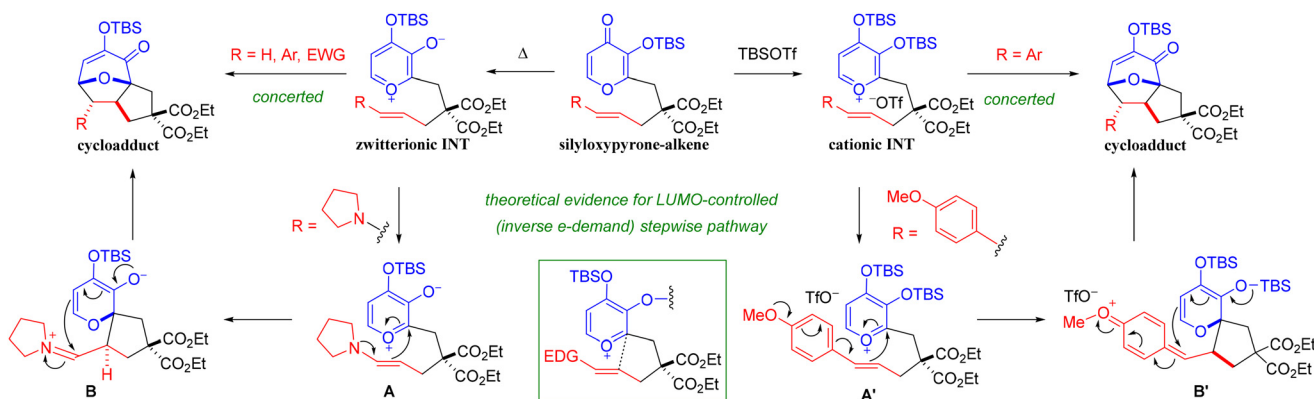


Fig. 8 TSs of substitute olefins: (a) nitro; (b) ketone;<sup>7b</sup> (c) ester; (d) H;<sup>7b</sup> (e) amine<sup>7b</sup> (TBS only for simplicity).

Comparison of previously calculated transition states<sup>7b</sup> for TBS variants with the newly calculated<sup>12</sup> enoate **2f** and nitro-ene **2m** reveals an interesting trend (Fig. 8). The terminal olefin **1a** is the closest to a synchronous concerted transition state **2a** with an energy barrier of 25.9 kcal mol<sup>-1</sup>. As electron-deficient substituents are introduced, the energy decreases and the mechanism shifts to concerted, but asynchronous along the following trend: enoate **2f** (23.4 kcal mol<sup>-1</sup>), enone **2k** (23.1 kcal mol<sup>-1</sup>), and nitro-ene **2m** (21.6 kcal mol<sup>-1</sup>). This trend correlates to experimental results in which more electrophilic dipolarophiles react faster than the terminal olefin **1a** (cf. Table 1). However, enamine **1o**, which was far more reactive experimentally (cf. Scheme 3), was predicted to be stepwise with an initial rate-determining transition state **2o** energy of 19.7 kcal mol<sup>-1</sup> followed by the second step which is only slightly lower in energy (18.8 kcal mol<sup>-1</sup>).<sup>7b</sup> Interestingly, nitro-ene **2m** is not quite electrophilic enough to promote formation of an analogous stepwise process with an anionic intermediate, but decreased bond lengths suggest that the transition state structure is progressively more asynchronous as the electron withdrawing ability of the substituent increases.

Based on these experiments and calculations, a unified mechanistic pathway is envisioned for both modes of activation (Scheme 5). Silyloxyprones can be activated by either thermal or Lewis acid-mediated (*i.e.* TBSOTf) conditions. Thermal activation with either TBS or TBDPS as transfer group promotes the formation of zwitterionic oxidopyrylium intermediates and can be achieved at temperatures as low as 0 °C in the case of electron-rich enamines (cf. Scheme 3). Ample evidence suggests that the TBDPS transfer group enhances the rate as compared to the TBS, but only for less polarized alkenes (*i.e.* terminal **1b** and styrenes **1q-z**). Likely this is due to an entropic effect that results from steric interactions of the TBDPS and the diester functionality leading to slightly lower energy barriers for cycloaddition. When the alkenes are more polarized, however, the dipolarophile substituent effect is more significant than this TBDPS acceleration and lowers the activation energy regardless. By contrast, TBSOTf promotes the formation of a cationic oxidopyrylium intermediate, which proceeds more rapidly in the case of electron-rich methoxy styrenes (cf. Tables 3 and 4). Both intermediates (*i.e.* zwitterionic or cationic) readily undergo concerted (5 + 2) cycloaddition



Scheme 5 Unified mechanism for thermal (TBS only for simplicity) and TBSOTf-mediated (5 + 2) cycloadditions.



(synchronous or asynchronous depending on the dipolarophile substituent) with neutral or electron-deficient dipolarophiles. However, quantum chemical calculations revealed evidence of LUMO-controlled, inverse electron demand stepwise pathways for electron-rich dipolarophiles for each set of activation parameters. Hammett plots also afforded crucial insight into both sets of conditions (*cf.* Fig. 1–4). In the case of the thermal-mediated zwitterionic-based cycloadditions, neutral alkenes were the least reactive, whereas both electron-deficient and electron-rich dipolarophiles were more reactive thus providing non-linear free energy relationships indicative of a change in mechanism. Hammett plots of the TBSOTf-mediated cycloadditions, however, revealed linear free energy relationships that are more in-line with a consistent mechanism throughout the reaction.

## Conclusions

Silyloxyprone-based (5 + 2) cycloadditions were investigated using both thermal and TBSOTf-mediated processes that revealed similarities and differences between these modes of activation. Thermal-mediated (5 + 2) cycloaddition proceeds through a zwitterionic oxidopyrylium intermediate, whereas TBSOTf-mediated (5 + 2) cycloaddition proceeds *via* cationic, bis-silylated intermediates. Qualitative rate studies, Hammett plots, and quantum calculations combined to illustrate a dichotomy between these two pathways. In the case of thermally induced variants with both TBS and TBDPS, both electron-deficient and electron-rich dipolarophiles were more reactive than neutral alkenes thus providing evidence for ambident zwitterionic oxidopyrylium intermediates. Several examples reveal that the TBDPS lowers the activation barrier, but only for less polarized olefins. Although most thermal-initiated reactions were concerted, theoretical evidence for a stepwise reaction pathway of electron-rich enamines was predicted. In TBSOTf-mediated cycloadditions, by contrast, electron-rich dipolarophiles are the most reactive and electron-deficient dipolarophiles are the least reactive. This observation is suggestive of cationic intermediates that demonstrate a more linear free energy relationship. A stepwise reaction pathway of the electron-donating methoxy styrene was also predicted with DFT. Overall, several dipolarophiles were investigated utilizing both modes of activation to probe the range of reactivity, which revealed a variety of mechanistic nuances between concerted and stepwise borderlands. A deep appreciation of these important mechanistic details is enabling opportunities to discover novel transformations to be reported in due course.

## Author contributions

The manuscript was written through contributions of all authors. A. J. Y., S. N. R., and W. G. contributed equally to this research. All authors have given approval to the final version of the manuscript.

## Conflicts of interest

There are no conflicts to declare.

## Data availability

The data supporting this article have been included as part of the supplementary information (SI). See DOI: <https://doi.org/10.1039/d6ob00305b>.

All structures are available in the ioChem-BD repository: <https://doi.org/10.19061/iochem-bd-6-585>.

## Acknowledgements

Acknowledgment is made to the National Science Foundation: individual research awards (CHE-1954588 and CHE-2350125) and XSEDE program for computational resources.

## References

- (a) N. Nishiwaki, *Methods and Applications of Cycloaddition Reactions in Organic Synthesis*, Wiley-VCH, Weinheim, 2014; (b) S. Kobayashi and K. A. Jørgensen, *Cycloaddition Reactions in Organic Chemistry*, Wiley-VCH, Weinheim, 2002; (c) W. Carruthers, *Cycloaddition Reactions in Organic Chemistry*, Tetrahedron Organic Chemistry, Pergamon, Oxford, 1990, vol. 8.
- (a) L. P. Bejcek and R. P. Murelli, Oxidopyrylium [5 + 2] cycloaddition chemistry: Historical Perspective and recent advances (2008–2018), *Tetrahedron*, 2018, **74**, 2501–2521; (b) V. Singh, U. M. Krishna, Vikrant and G. K. Trivedi, Cycloaddition of oxidopyrylium species in organic synthesis, *Tetrahedron*, 2008, **64**, 3405–3428; (c) J. L. Mascareñas, The [5 + 2] Cycloaddition Chemistry of  $\beta$ -Alkoxy- $\gamma$ -pyrones, *Adv. Cycloaddit.*, 1999, **6**, 1–54.
- J. B. Hendrickson and J. S. Farina, A New 7-Ring Cycloaddition Reaction, *J. Org. Chem.*, 1980, **45**, 3359–3361.
- P. G. Sammes and L. J. Street, Intramolecular Cycloadditions with Oxidopyrylium Ylides, *J. Chem. Soc., Chem. Commun.*, 1982, 1056–1057.
- (a) A. Rumbo, A. Mouriño, L. Castedo and J. L. Mascareñas, 3-Hydroxy-4-Pyrones as Precursors of 4-Methoxy-3-Oxidopyridinium Ylides. An Expedient Entry to Highly Substituted 8-Azabicyclo[3.2.1]octanes, *J. Org. Chem.*, 1996, **61**, 6114–6120; (b) A. Rumbo, L. Castedo, A. Mouriño and J. L. Mascareñas, Temporary Tethering Strategies for [5 + 2] Pyrone-Alkene Cycloadditions, *J. Org. Chem.*, 1993, **58**, 5585–5586; (c) P. A. Wender and J. L. Mascareñas, Preparation and Cycloadditions of a 4-Methoxy-3-Oxidopyrylium Ylid: A Reagent for the Synthesis of Highly Substituted Seven-Membered Rings and Tetrahydrofurans, *Tetrahedron Lett.*, 1992, **33**, 2115–2118; (d) P. A. Wender and F. E. McDonald, Studies on Tumor Promoters. 9. A Second-Generation Synthesis of Phorbol, *J. Am. Chem. Soc.*, 1990,



- 112, 4956–4958; (e) P. A. Wender and J. L. Mascareñas, Studies on Tumor Promoters. 11. A New [5 + 2] Cycloaddition Method and its Application to the Synthesis of BC Ring Precursors of Phoboids, *J. Org. Chem.*, 1991, **56**, 6267–6269.
- 6 (a) L. Yang, K. L. Chan, K. K. Cheung, P. Chiu, Z. Lin and J. Sun, Enantioselective type II intramolecular [5 + 2] cycloadditions of oxidopyrylium ylides using chiral-phosphoric-acid catalysis, *Nat. Synth.*, 2025, **4**, 1223–1231; (b) A. K. Ghosh and M. Yadav, Highly Diastereoselective Intramolecular Asymmetric Oxidopyrylium-olefin [5 + 2] Cycloaddition and Synthesis of 8-Oxabicyclo[3.2.1]oct-3-enone Containing Ring Systems, *J. Org. Chem.*, 2021, **86**, 8127–8142; (c) L. Zhang, Q. Shi, T. Cao and S. Zhu, Catalytic regio- and stereoselective intermolecular [5 + 2] cycloaddition via conjugative activation of oxidopyrylium, *Chem. Commun.*, 2020, **56**, 9533–9536; (d) C. Zhao, D. A. Glazier, D. Yang, D. Yin, I. A. Guzei, M. M. Aristov, P. Liu and W. Tang, Intermolecular Regio- and Stereoselective Hetero-[5 + 2] Cycloaddition of Oxidopyrylium Ylides and Cyclic Imines, *Angew. Chem., Int. Ed.*, 2019, **58**, 887–891; (e) Y. Toda, M. Shimizu, T. Iwai and H. Suga, Triethylamine Enables Catalytic Generation of Oxidopyrylium Ylides for [5 + 2] Cycloadditions with Alkenes: An Efficient Entry to 8-Oxabicyclo[3.2.1]octane Frameworks, *Adv. Synth. Catal.*, 2018, **360**, 2377–2381; (f) H. Suga, T. Iwai, M. Shimizu, K. Takahashi and Y. Toda, Efficient generation of an oxidopyrylium ylide using a Pd catalyst and its [5 + 2] cycloadditions with several dipolarophiles, *Chem. Commun.*, 2018, **54**, 1109–1112; (g) K. N. Fuhr, D. R. Hirsch, R. P. Murelli and S. E. Brenner-Moyer, Catalytic Enantioselective Intermolecular [5 + 2] Dipolar Cycloadditions of a 3-Hydroxy-4-pyrone-Derived Oxidopyrylium Ylide, *Org. Lett.*, 2017, **19**, 6356–6359; (h) S. M. Wilkerson-Hill, S. Sawano and R. Sarpong, Bis(1-cyanovinyl acetate) Is a Linear Precursor to 3-Oxidopyrylium Ions, *J. Org. Chem.*, 2016, **81**, 11132–11144; (i) M. P. D’Erasmus, C. Meck, C. A. Lewis and R. P. Murelli, Discovery and Development of a Three-Component Oxidopyrylium [5 + 2] Cycloaddition, *J. Org. Chem.*, 2016, **81**, 3744–3751; (j) A. Orue, U. Uria, E. Reyes, L. Carrillo and J. L. Vicario, Catalytic Enantioselective [5 + 2] Cycloaddition between Oxidopyrylium Ylides and Enals under Dienamine Activation, *Angew. Chem., Int. Ed.*, 2015, **54**, 3043–3046; (k) G. Mei, X. Liu, C. Qiao, W. Chen and C.-C. Li, Type II Intramolecular [5 + 2] Cycloaddition: Facile Synthesis of Highly Functionalized Bridged Ring Systems, *Angew. Chem., Int. Ed.*, 2015, **54**, 1754–1758; (l) M. R. Witten and E. N. Jacobsen, Catalytic Asymmetric Synthesis of 8-Oxabicyclooctanes by Intermolecular [5 + 2] Pyrylium Cycloadditions, *Angew. Chem., Int. Ed.*, 2014, **53**, 5912–5916; (m) K. Tchabanenko, C. Sloan, Y.-M. Bunetel and P. Mullen, Diastereoselective 1,3-dipolar cycloaddition of Pyrylium ylides with chiral enamides, *Org. Biomol. Chem.*, 2012, **10**, 4215–4219; (n) N. Z. Burns, M. R. Witten and E. N. Jacobsen, Dual Catalysis in Enantioselective Oxidopyrylium-Based [5 + 2] Cycloadditions, *J. Am. Chem. Soc.*, 2011, **133**, 14578–14581; (o) N. Ohmori, M. Yoshimura and K. Ohkata, Asymmetric Induction in Intramolecular [5 + 2] Cycloaddition of 2-(4-Alkenyl)-5-Benzoyloxy(or 5-Silyloxy)-4-Pyrones Involving Migration of the Pyrone O-5 Group to O-4, *Heterocycles*, 1997, **45**, 2097–2100.
- 7 (a) S. N. Angles, W. Guo, K. Darko, M. Erzuah, K. G. Pauley, I. E. Promise, J. R. Goodell, D. J. Tantillo and T. A. Mitchell, Net Intermolecular Silyloxy-pyrone-based (5 + 2) Cycloadditions Utilizing Amides as Enabling and Cleavable Tethers, *Org. Lett.*, 2023, **25**, 7137–7141; (b) A. J. Youman, S. N. Rokey, J. P. Grabowski, W. Guo, Q. Sun, S. N. Angles, J. R. Goodell, D. J. Tantillo and T. A. Mitchell, Experimental and Theoretical Investigation of the Synchronicity of Ambident Silyloxy-pyrone-Based (5 + 2) Cycloadditions, *J. Org. Chem.*, 2023, **88**, 5972–5981; (c) S. I. Corrie, A. C. Pearce, J. P. Grabowski, K. A. Randolph, W. Guo, D. J. Tantillo and T. A. Mitchell, Boron-tethered oxidopyrylium-based [5 + 2] cycloadditions, *Tetrahedron Lett.*, 2022, **107**, 154094; (d) Y. Lu and D. J. Tantillo, Comparison of (5 + 2) Cycloadditions Involving Oxidopyrylium and Oxidopyridinium Ions – Relative Reactivities, *J. Org. Chem.*, 2021, **86**, 8652–8659; (e) S. N. Rokey, J. A. Simanis, C. M. Law, S. Pohani, S. Willens Behrends, J. J. Bulandr, G. M. Ferrence, J. R. Goodell and T. A. Mitchell, Intramolecular asymmetric oxidopyrylium-based (5 + 2) cycloadditions, *Tetrahedron Lett.*, 2020, **61**, 152377; (f) J. P. Grabowski, G. M. Ferrence and T. A. Mitchell, Efforts toward the total synthesis of (±)-toxicodenane A utilizing an oxidopyrylium-based [5 + 2] cycloaddition of a silicon-tethered BOC-pyranone, *Tetrahedron Lett.*, 2020, **61**, 152324; (g) J. J. Bulandr, J. P. Grabowski, C. M. Law, J. L. Shaw, J. R. Goodell and T. A. Mitchell, Investigation of Transfer Group, Tether Proximity, and Alkene Substitution for Intramolecular Silyloxy-pyrone-Based (5 + 2) Cycloadditions, *J. Org. Chem.*, 2019, **84**, 10306–10320; (h) R. H. Kaufman, C. M. Law, J. A. Simanis, E. L. Woodall, C. R. Zwick III, H. B. Wedler, P. Wendelboe, C. G. Hamaker, J. R. Goodell, D. J. Tantillo and T. A. Mitchell, Oxidopyrylium-Alkene (5 + 2) Cycloaddition Conjugate Addition Cascade (C3) Sequences: Scope, Limitation, and Computational Investigations, *J. Org. Chem.*, 2018, **83**, 9818–9838; (i) J. A. Simanis, C. M. Law, E. L. Woodall, C. G. Hamaker, J. R. Goodell and T. A. Mitchell, Investigation of Oxidopyrylium-Alkene [5 + 2] Cycloaddition Conjugate Addition Cascade (C3) Sequences, *Chem. Commun.*, 2014, **50**, 9130–9133; (j) E. L. Woodall, J. A. Simanis, C. G. Hamaker, J. R. Goodell and T. A. Mitchell, Unique Reactivity of *anti*- and *syn*-Acetoxypyranones en route to Oxidopyrylium Intermediates Leading to a Cascade Process, *Org. Lett.*, 2013, **15**, 3270–3273; (k) S. C. Wang and D. J. Tantillo, Theoretical Studies on Synthetic and Biosynthetic Oxidopyrylium-Alkene Cycloadditions: Pericyclic Pathways to Intricarene, *J. Org. Chem.*, 2008, **73**, 1516–1523.
- 8 (a) N. Wang, Y. Bai, Q. Zeng, T. Zhang and J. Deng, Recent progress of [5 + 2] cycloaddition reactions in natural



- product synthesis, *Nat. Prod. Rep.*, 2025, **42**, 1755–1785; (b) K. Gao, Y.-G. Zhang, Z. Wang and H. Ding, Recent development on the (5 + 2) cycloadditions and their application in natural product synthesis, *Chem. Commun.*, 2019, **55**, 1859–1878; (c) X. Liu, Y.-J. Hu, J.-H. Fan, J. Zhao, S. Li and C.-C. Li, Recent synthetic studies toward natural products via, (5 + 2) cycloaddition reactions, *Org. Chem. Front.*, 2018, **5**, 1217–1228; (d) K. E. O. Ylijoki and J. M. Stryker, (5 + 2) Cycloaddition Reactions in Organic and Natural Product Synthesis, *Chem. Rev.*, 2013, **113**, 2244–2266.
- 9 (a) A. Aimon, G. Karageorgis, J. Masters, M. Dow, P. G. E. Craven, M. Ohsten, A. Willaume, R. Morgentin, N. Ruiz-Llamas, H. Lemoine, T. Kalliokoski, A. J. Eatherton, D. J. Foley, S. P. Marsden and A. Nelson, Realisation of small molecule libraries based on frameworks distantly related to natural products, *Org. Biomol. Chem.*, 2018, **16**, 3160–3167; (b) C. V. Credille, B. L. Dick, C. N. Morrison, R. W. Stokes, R. N. Adamek, N. C. Wu, I. A. Wilson and S. M. Cohen, Structure-Activity Relationships in Metal-Binding Pharmacophores for Influenza Endonuclease, *J. Med. Chem.*, 2018, **61**, 10206–10217; (c) D. R. Hirsch, D. V. Schiavone, A. J. Berkowitz, L. A. Morrison, T. Masaoka, J. A. Wilson, E. Lomonosova, H. Zhao, B. S. Patel, S. H. Datla, S. G. Hoft, S. J. Majidi, R. K. Pal, E. Gallicchio, L. Tang, J. E. Tavis, S. F. J. Le Grice, J. A. Beutler and R. P. Murelli, Synthesis and biological assessment of 3,7-dihydroxytropolones, *Org. Biomol. Chem.*, 2018, **16**, 62–69; (d) D. J. Foley, P. G. E. Craven, P. M. Collins, R. G. Doveston, A. Aimon, R. Talon, I. Churcher, F. von Delft, S. P. Marsden and A. Nelson, *Chem. – Eur. J.*, 2017, **23**, 15227–15232; (e) T. Masaoka, H. Zhao, D. R. Hirsch, M. P. D'Erasmus, C. Meck, B. Varnado, A. Gupta, M. J. Meyers, J. Baines, J. A. Beutler, R. P. Murelli, L. Tang and S. F. J. Le Grice, Characterization of the C-Terminal Nuclease Domain of Herpes Simplex Virus pUL15 as a Target of Nucleotidyltransferase Inhibitors, *Biochemistry*, 2016, **55**, 809–819.
- 10 (a) R. J. Zaragoza, M. J. Aurell and L. R. Domingo, The role of the transfer group in the intramolecular (5 + 2) cycloadditions of substituted  $\beta$ -hydroxy- $\gamma$ -pyrones: a DFT analysis, *J. Phys. Org. Chem.*, 2005, **18**, 610–615; (b) F. Lopez, L. Castedo and J. L. Mascarenas, A Theoretical Rationalization of the Asymmetric Induction in Sulfinyl-Directed [5C + 2C] Intramolecular Cycloadditions, *J. Org. Chem.*, 2003, **68**, 9780–9786; (c) L. R. Domingo and R. J. Zaragoza, Toward an Understanding of the Mechanisms of the Intramolecular (5 + 2) Cycloaddition Reaction of  $\gamma$ -Pyrones Bearing Tethered Alkenes. A Theoretical Study, *J. Org. Chem.*, 2000, **65**, 5480–5486.
- 11 D. J. Tantillo, Recent Excursions to the Borderlands between the Realms of Concerted and Stepwise: Carbocation Cascades in Natural Products Biosynthesis, *J. Phys. Org. Chem.*, 2008, **21**, 561–570.
- 12 See electronic supporting information.
- 13 C. Hansch, A. Leo and R. W. Taft, A Survey of Hammett Substituent Constants and Resonance and Field Parameters, *Chem. Rev.*, 1991, **91**, 165–195.
- 14 J. M. Crawford, C. Kingston, F. D. Toste and M. S. Sigman, Data Science Meets Physical Organic Chemistry, *Acc. Chem. Res.*, 2021, **54**, 3136–3148.
- 15 S. Grimme, Exploration of Chemical Compound, Conformer, and Reaction Space with Meta-Dynamics Simulations Based on Tight-Binding Quantum Chemical Calculations, *J. Chem. Theory Comput.*, 2019, **15**, 2847–2862.
- 16 M. J. Frisch, G. W. Trucks, H. B. Schlegel, G. E. Scuseria, M. A. Robb, J. R. Cheeseman, G. Scalmani, V. Barone, G. A. Petersson, H. Nakatsuji, X. Li, M. Caricato, A. V. Marenich, J. Bloino, B. G. Janesko, R. Gomperts, B. Mennucci, H. P. Hratchian, J. V. Ortiz, A. F. Izmaylov, J. L. Sonnenberg, D. Williams-Young, F. Ding, F. Lipparini, F. Egidi, J. Goings, B. Peng, A. Petrone, T. Henderson, D. Ranasinghe, V. G. Zakrzewski, J. Gao, N. Rega, G. Zheng, W. Liang, M. Hada, M. Ehara, K. Toyota, R. Fukuda, J. Hasegawa, M. Ishida, T. Nakajima, Y. Honda, O. Kitao, H. Nakai, T. Vreven, K. Throssell, J. A. Montgomery Jr., J. E. Peralta, F. Ogliaro, M. J. Bearpark, J. J. Heyd, E. N. Brothers, K. N. Kudin, V. N. Staroverov, T. A. Keith, R. Kobayashi, J. Normand, K. Raghavachari, A. P. Rendell, J. C. Burant, S. S. Iyengar, J. Tomasi, M. Cossi, J. M. Millam, M. Klene, C. Adamo, R. Cammi, J. W. Ochterski, R. L. Martin, K. Morokuma, O. Farkas, J. B. Foresman and D. J. Fox, *Gaussian 16, Revision A.03*, Gaussian, Inc., Wallingford CT, 2016.
- 17 S. Grimme, Density functional theory with London dispersion corrections, *Wiley Interdiscip. Rev.: Comput. Mol. Sci.*, 2011, **1**, 211–228.
- 18 (a) Y. Zhao and D. G. Truhlar, The M06 suite of density functionals for main group thermochemistry, thermochemical kinetics, noncovalent interactions, excited states, and transition elements: Two new functionals and systematic testing of four M06-class functionals and 12 other functionals, *Theor. Chem. Acc.*, 2006, **120**, 215–241; (b) Y. Zhao and D. G. Truhlar, Construction of a generalized gradient approximation by restoring the density-gradient expansion and enforcing a tight Lieb–Oxford bound, *J. Chem. Phys.*, 2008, **128**, 184109–184118.
- 19 (a) R. Krishnan, J. S. Binkley, R. Seeger and J. A. Pople, Self-consistent molecular orbital methods. XX. A basis set for correlated wave functions, *J. Chem. Phys.*, 1980, **72**, 650–654; (b) A. V. Marenich, C. J. Cramer and D. G. Truhlar, Universal Solvation Model Based on Solute Electron Density and on a Continuum Model of the Solvent Defined by the Bulk Dielectric Constant and Atomic Surface Tensions, *J. Phys. Chem. B*, 2009, **113**, 6378–6396.

